Ferromagnetism on a paramagnetic host background in cobalt-doped Bi_2Se_3 topological insulator*

Zhang Min(张 敏)[a], Lü Li(吕 莉)[a], Wei Zhan-Tao(魏占涛)[a], Yang Xin-Sheng(羊新胜)[a]†, and Zhao Yong(赵 勇)[a,b]

[a] Key Laboratory of Advanced Technology of Materials of Ministry of Education, Superconductor and New Energy R&D Center, Southwest Jiaotong University, Chengdu 610031, China

[b] Superconductivity Research Group, School of Materials and Engineering, University of New South Wale, Sydney, 2052 NSW, Australia

(Received 10 November 2013; revised manuscript received 22 January 2014; published online 29 May 2014)

Cobalt-doped Bi_2Se_3 topological insulators have been grown though melt-grown reaction. The Bi_2Se_3 matrix is diamagnetic and doped sample is a superposition of ferromagnetism (FM) and paramagnetism (PM) behavior at low temperature. The values of M_{Smol}, H_c, and M_r increase as the Co concentration increases. Two possible explanations have been proposed for the origin of ferromagnetism in Co-doped Bi_2Se_3. One is the magnetic ordering from nanoclusters of Co–Se compound in the crystals, and the other is Ruderman–Kittel–Kasuya–Yosida (RKKY) interaction between magnetic impurities.

Keywords: topological insulator (TI), ferromagnetism, Bi_2Se_3

PACS: 61.72.U–, 75.50.Gg, 75.50.Pp **DOI:** 10.1088/1674-1056/23/7/076104

1. Introduction

Three-dimensional (3D) topological insulators (TIs) are new materials that have a semiconductor gap in the bulk and nontrivial surface states (SSs) which are protected by time-reversal symmetry (TRS).[1–3] The protected surface states are believed to be robust to disorder, interactions, and thermal fluctuations, potentially leading to room-temperature spintronics technology.[4–8] An early report[9] pointed out that magnetic impurities can destroy the robust surface metallicity by interacting with the surface spin helicity and break TRS, whereas nonmagnetic impurities can maintain the robust surface massless Dirac cone. Theoretically, doping with transition metal elements can make the 3D topological insulators such as Bi_2Te_3, Bi_2Se_3, and Sb_2Te_3 to become magnetically ordered. In Fe- and Mn-substituted Bi_2Te_3,[10,11] Fe-substituted Sb_2Te_3[12] bulk single crystals and Cr-doped Bi_2Se_3 thin-film,[13] the ferromagnetism has been found. Magnetic impurities doped TIs have attracted extensive interest because they can affect surface states and induce many exotic phenomena. The intricate interplay between topological order and ferromagnetism is expected to provide a variety of unconventional effects that may lead to entirely new device paradigms. In this way the understanding of how magnetic properties behave in the presence of impurities is important not only for technological applications but also to fundamental physical questions. Recently, Li *et al.*[14] approved that ferromagnetism in Fe-doped Bi_2Se_3 is not induced by inclusions and may not be due to ferromagnetism of the bulk matrix. Highly Cr-doped (15%) Bi_2Se_3 bulk crystals were found to be antiferromagnetic.[15] Mn-doped single crystals of Bi_2Se_3 showed a spin-glass behavior.[16]

Magnetic properties in TIs have not yet been fully understood and still seem contradictory, and experimental studies of such phenomena are still at a nascent stage. In this paper, the influence of Co concentration x on magnetic properties of $Co_xBi_{2-x}Se_3$ is reported. The origin of magnetism in our single crystals is also discussed.

2. Experimental

The single $Co_xBi_{2-x}Se_3$ ($x = 0$, 0.02, 0.06, 0.12) were grown by melting a stoichiometric mixture of high-purity (99.999%) bismuth, selenium and cobalt powders. The pellets were grinded and pressed in a glove box with a nitrogen atmosphere, and then sealed in evacuated quartz tube (10^{-5} torr). The quartz tubes were heated at 850 °C for 8 h, then the furnace was slowly cooled to 620 °C for 50 h and keeping at the temperature for 24 h. Finally, quenching was carried out in water.

The obtained crystals were characterized by X-ray diffraction (XRD, X'Pert Panalytical). Microstructure was examined by field emission scanning electron microscope (FE-SEM, JSM-7001 F). The concentration of Co was confirmed by inductively coupled plasma optical emission spectroscopy (ICP-OES iCAP 6000, Thermo Scientific). Magnetization

*Project supported by the Program of International S&T Cooperation (Grant No. 2013DFA51050), the National Magnetic Confinement Fusion Science Program of China (Grant No. 2011GB112001), the Science Foundation of Sichuan Province, China (Grant Nos. 2011JY0031 and 2011JY0130), the National Natural Science Foundation of China (Grant Nos. 51271155 and 51002125), and the Fundamental Research Funds for the Central Universities of China (Grant Nos. SWJTU2682013CX005 and SWJTU12CX018).

†Corresponding author. E-mail: xsyang@swjtu.edu.cn

© 2014 Chinese Physical Society and IOP Publishing Ltd

measurements were carried out in a physical property measurement system (PPMS, Quantum Design). Hall effect was measured to determine the carrier concentration via van der Pauw's method using an electrical measurement system (East Chenging ET9005).

3. Results and discussion

The XRD pattern scans of $Co_xBi_{2-x}Se_3$ crystals are shown in Fig. 1. The reflections were only from the (00L) family, confirming that the crystals are c axis oriented. The patterns show no traces of impurities. For $Co_xBi_{2-x}Se_3$, the lattice constant c varies from 28.64 Å for non-doped sample to 28.59 Å for $x = 0.12$ (see the inset I in Fig. 1). The crystal quality is deteriorated with increasing Co concentration. The lattice constant c of doped samples is lower than that of pure sample. According to the bonding model of Krebs, the alien atoms in tetradymite-type crystals are incorporated into the Bi sublattice.[17–19] The structure of Bi_2Se_3 is highly anisotropic with hexagonal layers, so it has a good toleration for alien atoms. The alien atoms are able to intercalate within the five individual atomic layers. The c parameter decreases monotonously with increasing Co doping content, as the atomic radius of Co (1.25 Å) is smaller than that of Bi (1.63 Å). A small amount of Co atoms are incorporated into a tetradymite structure by occupation of Bi lattice sites. The remaining Co atoms probably form interstitial atoms or ions within the layers of the crystal lattice, or with an incorporation of Co atoms or ions inside the van der Waals gap of the crystal structure. The lattice parameter c of Fe-doped samples is lower than pure sample, which has been reported in our previous work,[20] no matter enter the van der Waals gap or intercalate between the individual atomic layers. As known to all, Cu enters Bi_2Se_3 either as an intercalant in the van der Waals gaps or as a substitutional defect to replace Bi.[21] Lošták *et al.*[19] reported that Fe atoms are easy to occupy interstitial positions inside the layers. The cleavage faces of pure Bi_2Se_3 are flat and shiny. After being doped by Co, a small quantity of Co–Se nano-clusters are formed with the neighboring Se layers, as shown in the inset II of Fig. 1. According to EDX analysis, Co content in defects area is higher than that in normal area (without defects).

The susceptibility for $Co_xBi_{2-x}Se_3$ has been measured under an applied field of 3000 Oe from 300 K to 2 K. The zero-field cooling/field cooling (ZFC/FC) magnetization curves for all doped samples are an almost reversible cycle in the whole temperature range, which is typical for the paramagnetic (PM) materials.[22] Figure 2 presents FC temperature-dependent magnetization curves, and M–T curves for $Co_xBi_{2-x}Se_3$. Pure Bi_2Se_3 shows a diamagnetic behavior with magnetic susceptibility $\chi_0 = -8.22 \times 10^{-5}$ emu/mol. For cobalt doped Bi_2Se_3 single crystal, an overall behavior closely resembling a paramagnet, which can be explained by the cobalt entering the structure and making Bi_2Se_3 a paramagnetic material.

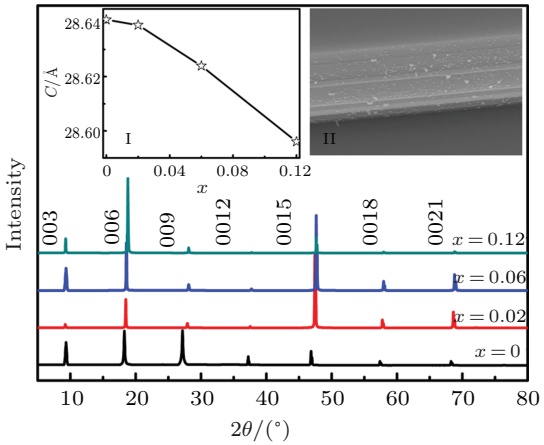


Fig. 1. (color online) X-ray diffraction patterns of $Co_xBi_{2-x}Se_3$ with different Co concentration ($x = 0$, 0.02, 0.06, and 0.12). Inset I: lattice parameters c as a function of Co concentration. Inset II: FESEM images for Co-doped sample with $x = 0.06$.

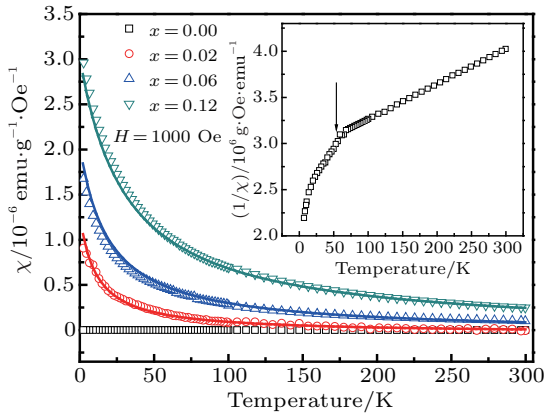


Fig. 2. (color online) Magnetic susceptibility versus temperature for $Co_xBi_{2-x}Se_3$ under applied magnetic field of 1000 Oe parallell to the c axis. Symbols represent the experimental data, and solid lines indicate the fitting curves. Inset: inverse magnetic susceptibility as a function of temperature for $Co_{0.12}Bi_{1.88}Se_3$, and the arrow indicates the presence of magnetic phase.

Table 1. Co concentration, carrier concentration, and fitting parameters of the Curie–Weiss analysis of $Co_xBi_{2-x}Se_3$ crystals.

x	C_{Co}/cm^{-3}	N/cm^{-3}	χ_0/emu·mol^{-1}	C/emu·K·g^{-1}·Oe^{-1}	θ/K	μ_{eff}	S
0.00	–	-1.12×10^{19}	-8.22×10^{-5}	–	–	–	–
0.02	3.539×10^{19}	-1.33×10^{19}	-7.64×10^{-5}	1.297×10^{-5}	−11.1	3.354	1.398
0.06	1.924×10^{20}	-1.63×10^{19}	-7.85×10^{-5}	6.614×10^{-5}	−17.4	3.247	1.199
0.12	2.903×10^{20}	-9.85×10^{18}	-8.01×10^{-5}	9.155×10^{-5}	−31.0	3.111	1.134

In the paramagnetic region, the experimental data of the samples can be fitted by the Curie–Weiss law:

$$\chi = \chi_0 + \frac{C}{T-\theta}, \tag{1}$$

where C, θ, and χ_0 are the Curie–Weiss constants, paramagnetic Currie temperature, and temperature-independent term. The fitted values are listed in Table 1, and the fitting lines are shown by solid curves in Fig. 2. The paramagnetic Curie temperatures are determined as negative values for all the samples, implying that an antiferromagnetic interaction is between the local electrons. The dependence of the Curie–Weiss constants on effective Bohr magneton number $\mu_{\rm eff}$ can be written as

$$C = \frac{N\mu_{\rm eff}^2\mu_{\rm B}^2}{3k_{\rm B}}. \tag{2}$$

The N is the concentration of Co ions obtained from the ICP-OES, $\mu_{\rm B}$ is the Bohr magneton, and $k_{\rm B}$ is the Boltzmann constant. The angular momentum quantum number J can be estimated from the following expression:

$$\mu_{\rm eff} = g\sqrt{J(J+1)}, \tag{3}$$

where $g = 2$ is the Lande factor and the angular momentum quantum number $J \approx S$ (orbital angular momentum is assumed to be quenched due to the crystal field of neighboring atoms).[12] The calculated spin values of S of all three samples range from 1 to 3/2. This suggests that the valence state of cobalt in the $Co_xBi_{2-x}Se_3$ crystals are Co^{3+} and Co^{2+}. The Co^{2+} ions are in high spin (HS) states with $S = 3/2$ and Co^{3+} ions are in intermediate spin (IS) state with $S = 1$.

A deviation from the expected linear behavior of the $1/\chi$ curve of $Co_{0.12}Bi_{1.88}Se_3$ crystals (inset of Fig. 2) is observed, suggesting the presence of magnetic phase. To verify the presence of the magnetic phase and the magnetic order, magnetization versus applied magnetic field curves for $Co_xBi_{2-x}Se_3$ has been measured at 12 K, as shown in Fig. 3. The black symbols present diamagnetic signals of pure Bi_2Se_3. With Co doping, there are clear hysteresis loops, which suggests the existence of FM state. It is noted that magnetization increases gradually with the Co concentration. The magnetization is the superposition of two contributions: a paramagnetic component characterized by an almost linear variation of M versus H at high fields, and a ferromagnetic component characterized by an irreversible behavior and a low coercive field. After subtraction of the paramagnetic signals from the total signals, hysteresis loops have been extracted from the experimental data. For all samples, a superposition of paramagnetic behavior and a ferromagnetic is evidenced, as shown in Figs. 4(a) and 4(b), respectively. Fe-doped Bi_2Se_3 exhibits diamagnetic background in the low temperature. In contrast, Co-doped Bi_2Se_3 in the low temperature range displays diamagnetic background. The paramagnetic background is assumed to be caused by the fact that Co ions are in the host matrix and the contribution of magnetic ions to the ferromagnetic ordering is very limited.

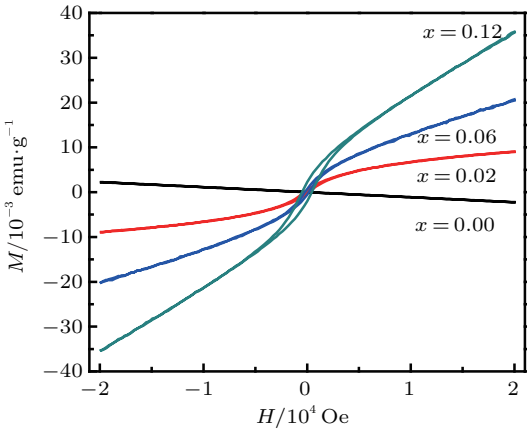


Fig. 3. (color online) Magnetization versus applied magnetic field for $Co_xBi_{2-x}Se_3$ measured at 12 K. There is obvious magnetic hysteresis in highly doped samples.

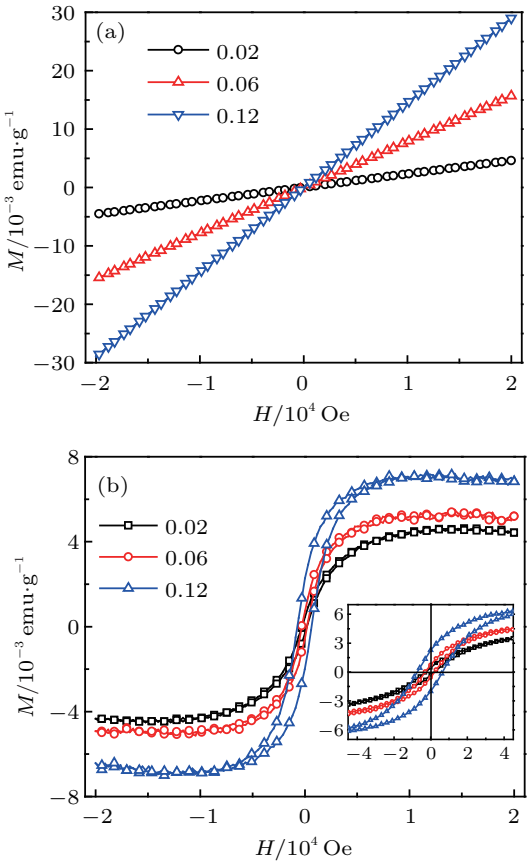


Fig. 4. (color online) (a) Paramagnetic contributions of the $Co_xBi_{2-x}Se_3$ crystals. (b) Hysteresis curves of the $Co_xBi_{2-x}Se_3$ crystals. Inset: enlarged view of the hysteresis cycles of $Co_xBi_{2-x}Se_3$ crystals.

The molar saturation magnetization $M_{\rm Smol}$ is deduced from the subtracted hysteresis loops. The magnetic saturation moment per cobalt ion is $0.011\mu_{\rm B}$–$0.04\mu_{\rm B}$, are listed in the Table 2, whereas $2.82\mu_{\rm B}$ is expected in a system where all of

the cobalt is fully aligned in the Co^{3+} state and assuming a total quenching of the orbital moment. This discrepancy points to the fact that not all Co contributes to the ferromagnetism, while some Co form other substance or exist in a different valence state than the expected Co^{3+}.[13] In other magnetic topological insulators, the value of M_{Smol} is $0.4\mu_B$ for Cr-doped Bi_2Se_3[22] and is $0.07\mu_B$ for Fe-doped Bi_2Se_3.[14] They are larger than the Co-doped Bi_2Se_3. In spite of very low amount of ferromagnetic ions in Bi_2Se_3, it is also possible to measure the coercivity H_c (Table 2). The details of loops at low fields for Co doping samples are plotted in the inset of Fig. 4(b). As the concentration of Co increases, the M_{Smol} values increase obviously. The coercive field H_c varies from 260 Oe for $x = 0.02$ to 730 Oe for $x = 0.12$, as the Co concentration increases. It is noted that the remanent magnetization M_r increases with the Co concentration. It can be supposed that ferromagnetism is closely related to Co concentration, based on the rising tendency of M_{Smol}, H_c, and M_r. The magnetism strongly depends on the Co content in our samples, while it does not depend on the Fe content in Fe-doped Bi_2Se_3.[13] The low M_{Smol} value could be ascribed to a low quantity of Co ions involving in ferromagnetic state, while most of them remain in a PM state.

Table 2. Remanent magnetization (M_r), saturation magnetization (M_{Smol}), and coercivity (H_c) for $Co_xBi_{2-x}Se_3$.

x	M_{Smol}		$M_r/10^{-3}$ emu·g^{-1}	H_c/Oe
0.02	4.55[a)]	0.040[b)]	0.747	260
0.06	5.17[a)]	0.015[b)]	0.743	312
0.12	6.99[a)]	0.011[b)]	2.343	730

[a)] in units of 10^{-3} emu/g, [b)] in units of μ_B per Co atom.

According to the magnetic moments of Co inclusions,[24] if the ferromagnetism comes from Co inclusions, the magnetic moment per atom in small clusters should equal or exceed the bulk value of $2.08 \pm 0.20\mu_B$ per atom. Thus, the formation of Co inclusions can be excluded the origin of FM, as the values of magnetic moments per atom for Co-doped Bi_2Se_3 are less than $0.04\mu_B$. In addition, since the M–T curve does not appear the "λ" shape, we conclude that the magnetic properties of the samples are not from the cobalt particles.[25] The samples of Co-doped Bi_2Se_3 are not diluted magnetic semiconductors (DMS), as the magnetic properties of DMS obviously depend on the carrier density.

Calculation of spin values of S suggests that Co^{3+} and Co^{2+} ions coexist in Co-doped Bi_2Se_3 crystals. Co^{2+} mainly forms Co–Se compounds, while Co^{3+} plays an important role for the increase in magnetic moment because of substitution effect. There are two possible explanations for the FM. Firstly, a small amount of ferromagnet of Co–Se compound was formed. The reported value of H_c for $CoSe_2$ nanocrystals is approximately 600 Oe[26] and has the same order of magnitude as our results. Hence, we think that some $CoSe_2$ nanocrystals exist in our Co-doped Bi_2Se_3 samples. Secondly, FM most probably originates from the certain concentration of magnetic atoms substitutes for the Bi. Ruderman–Kittel–Kasuya–Yosida (RKKY) interaction between magnetic impurities has been proposed to be responsible for the magnetic ordering of the substituted TIs. Schmidt *et al.*[27] argued that the Co–Co interaction favors an FM state based upon first-principles methods.

4. Summary

Cobalt-doped Bi_2Se_3 single crystals have been grown though melt-grown reaction. For Co doping samples, the M–T curve shows no hint of ferromagnetism down to 2 K. The ZFC/FC curves of all doped samples are an almost reversible cycle, which can be fitted by the Curie–Weiss law. Both the magnitude of the susceptibility and its increase with decreasing temperature are enhanced by increasing Co substitution. The $M(H)$ curve shows hysteresis for cobalt-doped Bi_2Se_3 single crystals at low temperature. Bi_2Se_3 matrix is diamagnetic and doped samples are a superposition of FM and PM behavior at 12 K. The values of M_{Smol}, H_c, and M_r increase with Co concentration, which implies that the magnetism is strongly dependent on the Co content. There are two possible explanations for the FM. Firstly, the bulk ferromagnetic behavior of Co-doped Bi_2Se_3 is due to nanoclusters of Co–Se compound in the crystals. Secondly, the Ruderman–Kittel–Kasuya–Yosida (RKKY) interaction between magnetic impurities favors the FM state.

References

[1] Qi X L and Zhang S C 2011 *Rev. Mod. Phys.* **82** 1057
[2] Roushan P, Seo J, Parker C V, Hor Y S, Hsieh D, Qian D, Richardella A, Hasan M Z, Cava R J and Yazdani A 2009 *Nature* **460** 1106
[3] Qi X L, Hughes T L and Zhang S C 2008 *Phys. Rev. B* **78** 195424
[4] Fu L and Kane C L 2009 *Phys. Rev. Lett.* **102** 216403
[5] Yu R, Zhang W, Zhang H J, Zhang S C, Dai X and Fang Z 2010 *Science* **329** 61
[6] Zhang H, Liu C X, Qi X L, Dai X, Fang Z and Zhang S C 2009 *Nat. Phys.* **5** 438
[7] Moore J E 2010 *Nature* **464** 194
[8] Xiu F X and Zhao T T 2013 *Chin. Phys. B* **22** 096104
[9] Chen Y L, Chu J H, Analytis J G, Liu Z K, Igarashi K, Kuo H H, Qi X L, Mo S K, Moore R G, Lu D H, Hashimoto M, Sasagawa T, Zhang S C, Fisher I R, Hussain Z and Shen Z X 2010 *Science* **329** 659
[10] Hor Y S, Roushan P, Beidenkopf H, Seo J, Qu D, Checkelsky J G, Wray L A, Hsieh D, Xia Y, Xu SY, Qian D, Hasan MZ, Ong N P, Yazdani A and Cava R J 2010 *Phys. Rev. B* **81** 195203
[11] Kulbachinskii V A, Kaminskii A Y, Kindo K, Narumi Y, Suga K, Lošťák P and Svanda P 2002 *Physica B* **311** 292
[12] Zhou Z H, Žabčík M, Lošťák P and Uher C 2006 *Appl. Phys.* **99** 043901
[13] Haazen P P J, Laloë J B, Nummy T J, Swagten H J M, Jarillo-Herrero P, Heiman D and Moodera J S 2012 *Appl. Phys. Lett.* **100** 082404
[14] Li H, Song Y R, Yao M Y, Zhu F F, Liu C H, Gao C L, Jia J F, Qian D, Yao X, Shi Y J and Wu D 2013 *J. Appl. Phys.* **113** 043926
[15] Choi Y H, Jo N H, Lee K J, Yoon J B, You C Y and Jung M H 2011 *J. Appl. Phys.* **109** 07E312

[16] Choi J, Lee H W, Kim B S, Park H, Choi S, Hong S and Cho S 2006 *J. Magn. Magn. Mater.* **304** e164
[17] Hor Y S, Richardella A, Roushan P, Xia Y, Checkelsky J G, Yazdani A, Hasan M Z, Ong N P and Cava R J 2009 *Phys. Rev. B* **79** 195208
[18] Wang Y L, Xu Y, Jiang Y P, Liu J W, Chang C Z, Chen M, Li Z, Song C L, Wang L L, He K, Chen X, Duan W H, Xue Q K and Ma X C 2011 *Phys. Rev. B* **84** 075335
[19] Lošťák P, Drašar Č, Klichová I, Navrátil J and Černohorský T 1997 *Phys. Stat. Sol.* **200** 289
[20] Lv L, Zhou D, Zhang M, Yang L, Yang X and Zhao Y 2013 *Mater. Lett.* **99** 118
[21] Kriener M, Segawa K, Ren Z, Sasaki S, Wada S, Kuwabata S and Ando Y 2011 *Phys. Rev. B* **84** 054513
[22] Cullity B D 1872 *Introduction to Magnetic Materials* (New York: Addison–Wesley)
[23] SongY R, Yang F, Yao M Y, Zhu F, Miao L, Xu J P, Wang M X, Li H, Yao X, Ji F, Qiao S, Sun Z, Zhang G B, Gao B, Liu C, Qian D, Gao C L and Jia J F 2012 *Appl. Phys. Lett.* **100** 242403
[24] Bucher J P, Douglass D C and Bloomfield L A 1991 *Phys. Rev. Lett.* **66** 23
[25] Song H Q, Chen Y X, Ren M J and Ji G 2005 *Acta Phys. Sin.* **54** 369 (in Chinese)
[26] Gao J, Zhang B, Zhang Xi and Xu B 2006 *Angew. Chem.* **18** 1242
[27] Schmidt T M, Miwa R H and Fazzio A 2011 *Phys. Rev. B* **84** 245418